

www.acsami.org Research Article

Tunable Photothermal Actuation Enabled by Photoswitching of Donor-Acceptor Stenhouse Adducts

Jaejun Lee,[§] Miranda M. Sroda,[§] Younghoon Kwon, Sara El-Arid, Serena Seshadri, Luke F. Gockowski, Elliot W. Hawkes, Megan T. Valentine,^{*} and Javier Read de Alaniz*



Cite This: ACS Appl. Mater. Interfaces 2020, 12, 54075-54082



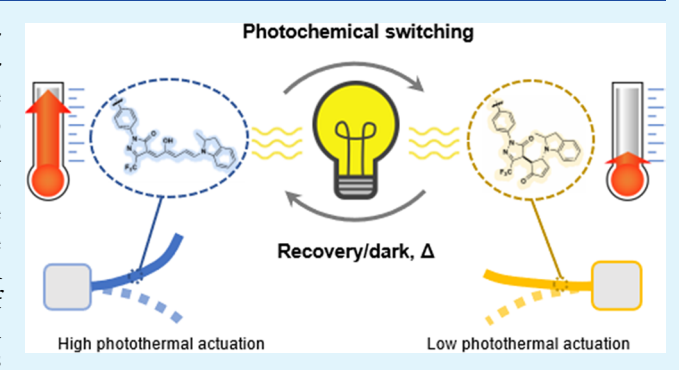
ACCESS

III Metrics & More

Article Recommendations

s Supporting Information

ABSTRACT: We report a visible light-responsive bilayer actuator driven by the photothermal properties of a unique molecular photoswitch: donor—acceptor Stenhouse adduct (DASA). We demonstrate a synthetic platform to chemically conjugate DASA to a load-bearing poly(hexyl methacrylate) (PHMA) matrix via Diels—Alder click chemistry that enables access to stimuli-responsive materials on scale. By taking advantage of the negative photochromism and switching kinetics of DASA, we can tune the thermal expansion and actuation performance of DASA—PHMA under constant light intensity. This extends the capabilities of currently available responsive soft actuators for which mechanical response is determined exclusively by light intensity and enables



the use of abundant broadband light sources to trigger tunable responses. We demonstrate actuation performance using a visible light-powered cantilever capable of lifting weight against gravity as well as a simple crawler. These results add a new strategy to the toolbox of tunable photothermal actuation by using the molecular photoswitch DASA.

KEYWORDS: donor—acceptor Stenhouse adducts, photoswitch, photothermal actuation, negative photochromism, light-responsive

■ INTRODUCTION

Developing stimuli-responsive agents that can trigger mechanical responses via environmental changes (e.g., temperature, humidity, 2,3 pH, 4 and light 5,6) is key to advancing the design and control of soft actuators for use in locomotive robots, artificial muscles, grippers, and oscillators. Light is advantageous as both an energy source and signal for high spatiotemporal resolution control due to its readily tunable intensity, spot size, and wavelength and the availability of remote control. Extensive use of light to achieve controlled actuation has been reported using photoresponsive agents, including photoswitching molecules, 11-13 carbon-based materials, 14,15 and gold nanoparticles. 16,17 In general, such actuators produce a single actuation mode under a single light intensity since the mechanical energy generation is determined exclusively by the amplitude of external stimuli. This prevents the performance of multiple tasks under constant illumination, such as sunlight and ambient light, where energy input cannot be easily "tuned". New materials capable of modulating performance using programmed logic under constant excitation are required.

Previous strategies for tunable actuation include the use of dynamic covalent networks, 9,18 chemical processing, 19 shadowing effects, 20–22 self-oscillating, 23 reconfigurable patterning, 24 and structural patterning 25,26 that often require prolonged processing. More recently, an elegant cooperative use of photochemical patterning and photothermal actuation in a

liquid crystalline network (LCN) has been developed.²⁷ This strategy relies on the molecular alignment of the azobenzenebased LCN: E/Z photoisomerization programs strain while red light irradiation of an anthraquinone dye triggers photothermal actuation. The absorption properties of the azobenzene photoswitch require the use of narrow-bandwidth (<100 nm) high-energy UV-light to embed programming logic via photoisomerization.²⁸ The challenge remains to design materials that leverage the cooperative use of photochemical and photothermal properties to tune actuation that operates with less harmful, abundant, and economically beneficial broadband light sources (i.e., halogen lamps, white LEDs, and sunlight). Achieving this would require moving away from traditional azobenzene-based stimuli-responsive materials and would move the field one step closer to actuators that can be powered by sunlight.

In this work, we aim to develop a load-bearing material that can respond to broadband visible light and empower tunable actuation. We enable tunability by exploiting a previously

Received: August 21, 2020 Accepted: October 29, 2020 Published: November 19, 2020





unexplored strategy that introduces cooperative photothermal actuation and photochemical control using negatively photochromic materials meaning that the photoproduct absorption shifts to the blue of the reactant absorption and thus does not absorb the exciting light. To achieve this, we leverage the intrinsic photochemical properties of donor—acceptor Stenhouse adducts (DASAs).^{29–31} DASAs have a high molar absorptivity in the open form (>100,000 M⁻¹ cm⁻¹), a colorless closed form, tunable kinetics, and adjustable absorption profiles in the visible to near-IR window for multiwavelength control.²⁹ We hypothesize that upon irradiation with visible light, the rapid photothermal energy conversion of DASAs can be harnessed to drive mechanical actuation, while the conversion from a highly absorbing colored form to a colorless and transparent form can switch off the photothermal sensitizer to enable photochemical control (Figure 1). The rapid photothermal heating enables the

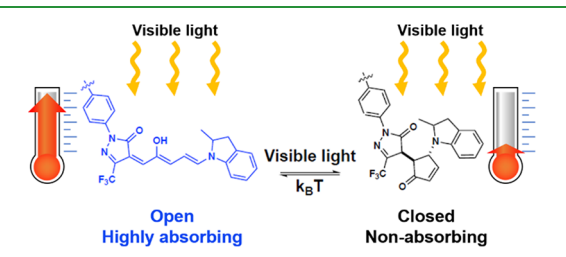


Figure 1. Structure and photoswitching of donor—acceptor Stenhouse adducts. The highly absorbing, colored open form empowers photothermal energy conversion, while the nonabsorbing, colorless closed form generates less heat upon irradiation providing control over the magnitude of actuation.

use of simple design principles including an amorphous structure and bilayer configuration, avoiding the complex processing step of molecular alignment of LCNs. The kinetics of these transitions can be controlled by the design of the photoswitch and physicochemical conditions. This allows photothermal actuation and photochemical control to occur on different timescales under constant external input, thereby enabling novel forms of tunability. We have recently demonstrated how the controllable photothermal properties, negative photochromism, and high molar absorptivity of DASAs could be leveraged to achieve self-regulating control of fluid motion. In conceptually related work, the use of switchable tungsten (VI) oxide nanoparticles, WO₃, has been recently used as a photothermal sensitizer for high color quality 3D printing. The supplies the structure of the supplies of the supplie

Herein, we report the development and use of a DASA—polymer conjugate in the solid state to enable tunable, load-bearing actuation to produce mechanical work. We demonstrate visible light-powered actuation performance with a cantilever capable of lifting a weight against gravity and a remotely powered and controlled crawler. Our results demonstrate the promise of this material design strategy for rapid and self-tunable photoinduced actuation using negatively photochromic, amorphous materials.

■ RESULTS

To construct the DASA—polymer conjugate and generate a negatively photochromic light-responsive bilayer actuator, we developed a synthetic strategy using Diels—Alder click chemistry (Figure 2).³⁸ This method overcomes many limitations of the current functionalization strategies that rely on DASA formation in the final step including long reaction times, incomplete functionalization, and multiple postpolymerization

steps. 34,39-41 We chemically conjugated the DASA molecules to the polymer backbone to provide more uniform dispersion and high thermal stability as compared to physical blending.⁴² Specifically, copolymers containing poly(hexyl methacrylate) (PHMA) and the functional monomer, norbornadiene methacrylate (NBD-MA), were synthesized using reversible addition-fragmentation chain transfer polymerization to generate 10 mol % NBD-PHMA. Hexyl methacrylate was chosen as a comonomer due to its optical transparency in the visible region⁴³ and mechanical properties.⁴⁴ A maleimide bearing a third-generation DASA-based photoswitch with a CF₃pyrazolone acceptor and a 2-methyl indoline donor was prepared (Figure 2a). This derivative was chosen due to its high molar absorptivity and enhanced dark equilibrium compared to prior generations³⁵ and "clicked" onto the polymer using tetrazine to initiate the cascading Diels-Alder reaction (Figure 2b). Detailed synthetic procedures and characterization results are shown in the Supporting Information. A target incorporation of 10 mol % DASA was chosen to provide sufficient photothermal heat generation to drive actuation, while enabling control of the switching kinetics to impart programm-¹H NMR and UV-vis spectroscopy were used to confirm DASA incorporation: a distinct DASA peak centered at ~648 nm was observed in both the DASA-maleimide and the 10 mol % DASA-PHMA samples (Figure 2c). Differential scanning calorimetry (DSC) of the DASA-PHMA conjugate indicated an increase in T_g from the parent polymer from -10 to 45 °C (Figure S1). The amorphous character was established by XRD and DSC (Figure S2).

To demonstrate light-driven motion using this photoresponsive material, a 20 mm × 1.5 mm bilayer actuator was prepared by drop casting (Figure 2d). In contrast to the aligned LCN systems that offer the ability to program complex 3D shape changes,²⁷ we initially explored the use of a DASA-PHMA polymer-based system in an amorphous bilayer in order to lift weight and generate work. Our use of amorphous fabrication techniques avoids the complexities of molecular alignment of LCNs, while also eliminating the need for thiol-Michael additions⁴⁶ and radical polymerizations⁴⁷ that are traditionally used for LCN preparation but are not compatible with DASA functionality. The fabrication method is straightforward: a thin film of DASA-PHMA was deposited (film thickness of ~10 µm) onto a commercially obtained polyimide (PI) film (thickness of $\sim 25 \mu m$) that serves as the inactive layer. The thickness was confirmed by scanning electron microscopy and optical microscopy (Figure 2e).

With access to the DASA-PHMA photoresponsive material, we set out to explore photothermally driven actuation using a bilayer DASA-PHMA/PI cantilever system (Figure 3) that takes advantage of the differences in thermal expansion caused by DASA-dependent heat generation to induce bending.⁴⁸ A light source (halogen lamp, EKE 150 W with a fiber optic illuminator) located above the cantilever directly illuminated the DASA-PHMA layer. A small weight was placed on the tip of the cantilever to evaluate the capability of the actuator to lift against gravity, thereby performing mechanical work (Figure 3a). For each experiment, the deflection of the cantilever tip was continuously recorded before, during, and after irradiation. Representative snapshot images of the motion are presented in Figure 3b; the dotted blue line indicates the initial cantilever position, which has bowed under the added weight at the tip. Upon illumination, an initial fast lifting motion was observed with a speed of ~1.8 mm/s for ~1 s, followed by a gradual

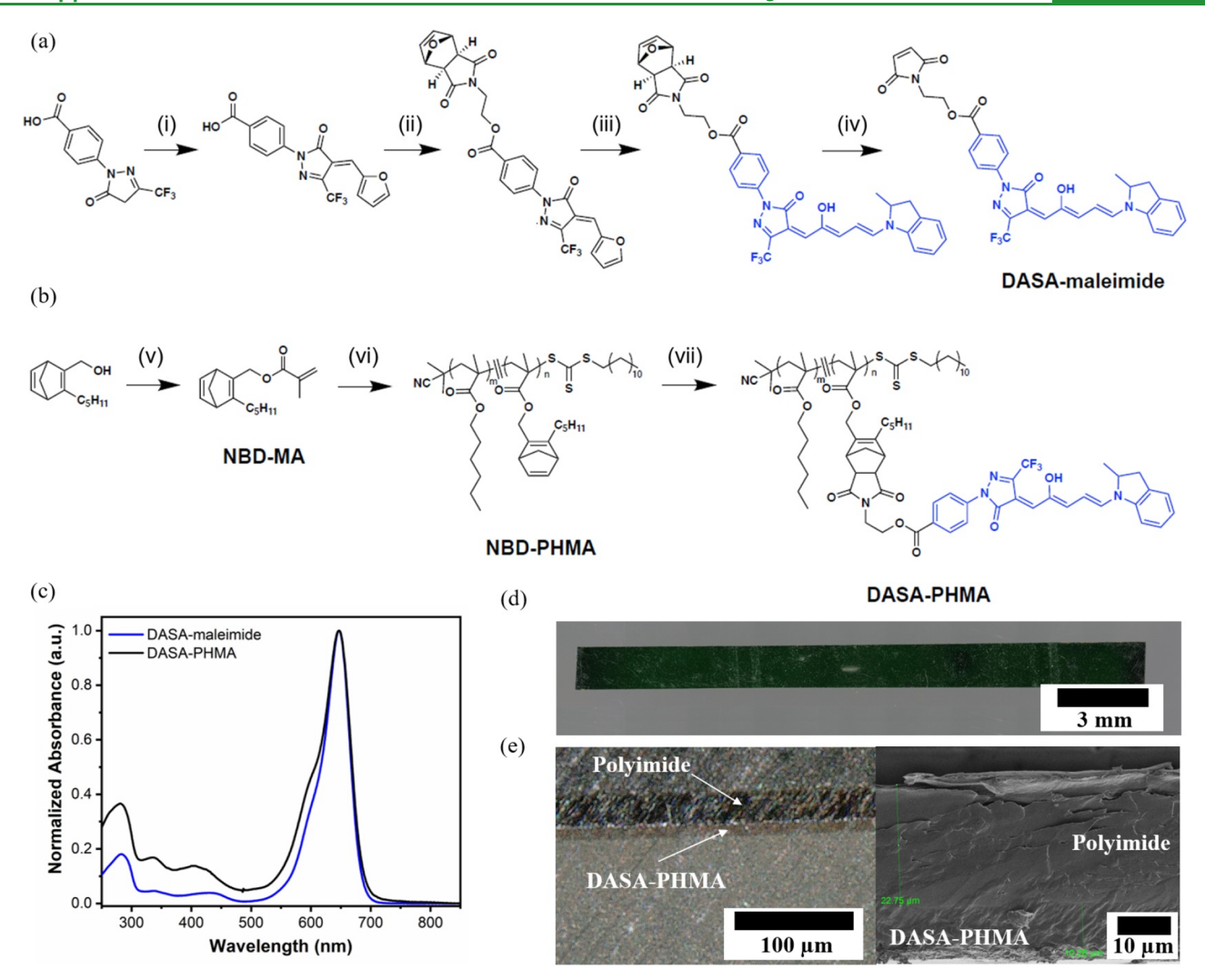


Figure 2. Molecular design and characterization of a photothermally responsive DASA polymer. Synthetic pathways for (a) DASA—maleimide and (b) DASA—PHMA by "clicking" DASA—maleimide onto NBD—PHMA using Diels—Alder chemistry. (c) DASA—maleimide and DASA—PHMA UV—vis spectra exhibit identical absorbance max at ~648 nm in solution (chloroform). (d) Photographic image of the bilayer specimen and (e) cross-sectional image of the bilayer (left) taken by an optical microscope and (right) an SEM image of the cross section.

slowing down of the cantilever as it reached steady-state deflection (Figure 3c). The peak deflection was achieved within $\sim\!1.5$ s of illumination, and once the light was turned off, the cantilever returned to its initial position on a similar timescale. The response time of the cantilever is similar to other photothermally actuating polymeric cantilevers. We assume that the fast response of the cantilever can be attributed to the fast temperature increase under light illumination but other factors such as light intensity, size, and radius of curvature of the cantilever might also play a role.

The beam dynamics appear to closely track the temperature change as measured using an IR camera (experimental details are provided in the Supporting Information), as expected for the photodriven asymmetric thermal expansion of the bilayer. This was further confirmed through thermal mechanical analysis. The linear coefficient of thermal expansion for DASA—PHMA was measured to be 9 times higher than that of PI (Figure S3) for temperatures ranging from 0 to 35 °C. As irradiance was increased, the average peak deflection and temperature increased proportionally (Figure 3d). As a further confirmation that the dominant mechanism of actuation is photothermal, we subjected a cantilever to a temperature ramp at a rate of 3 °C/

min using a temperature-controlled chamber and observed similar bending profiles as compared to those obtained via illumination at room temperature (Figure S4). Finally, upon investigation of the actuation in water, a highly effective heat dissipation medium, we observed very limited actuation with a peak deflection of ~ 0.3 mm in water versus ~ 4 mm in air (Figure S5). Taken together, these results support that photothermal heating is a main feature contributing to the deflection under light.

To evaluate the mechanical actuation performance of the cantilever, the mechanical work generated under illumination was measured by calculating the potential energy difference between the initial position and final position under peak deflection as a function of added weight (Figure 3e). We found that the work increased linearly with increasing weight and that the simple actuator could lift against gravity a weight up to 13 times that of the DASA–PHMA/PI cantilever alone. Note that we were unable to measure the maximum work capacity using the current setup due to low bending stiffness (17.5 N/m) of the current cantilever; heavier loads force the cantilever into a near vertical orientation, thereby bending it away from the light source and limiting the amount of light energy that can be

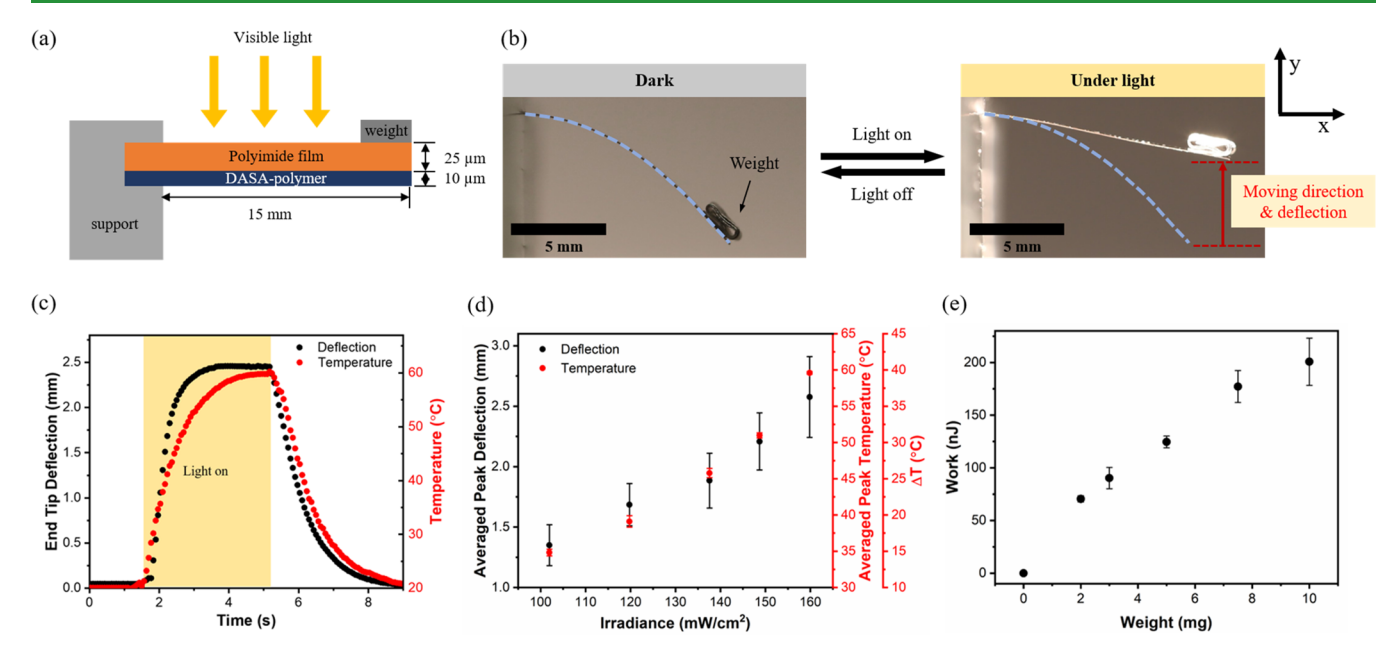


Figure 3. Photothermally powered DASA-PHMA/PI bilayer cantilever: actuation performance and temperature response. (a) Schematic of the experimental configuration. (b) Snapshot images showing that the cantilever lifts under light and drops when light is turned off. Weight is 5 mg. (c) Representative data traces showing tip deflection (y axis displacement) and temperature as a function of time (5 mg weight, 160 mW/cm² irradiance, halogen lamp). (d) Averaged peak deflection (with 5 mg weight) and averaged peak temperature are plotted as a function of irradiance; both values increase linearly with irradiance. (e) Photothermally driven mechanical work calculated by $m_0 g \Delta h$, where m_0 is the mass of the added weight at the tip, g is the acceleration due to gravity, and Δh is the maximal change in tip position before and after illumination plotted as a function of added weight (red arrow in panel b).

absorbed as compared to cantilevers bearing lighter loads. Future directions will explore modifying the bilayer thickness and design to determine the maximum work capacity of the actuator. Finally, the light-driven bending action is robust and repeatable, as evident through a series of 30 illumination—dark cycles using a 5 mg weight at the cantilever tip (Figure S6), although a slight decrease in peak deflection after several illumination-dark cycles was observed. We speculate that slow switching from the open, highly absorbing form to the closed, transparent, and less absorbing form of DASA results in the gradual performance decline.³⁴ The full conversion time of the 10 μ m-thick DASA-PHMA specimen under 160 mW/cm² light illumination is ~400 s, which is significantly longer than the photothermal actuation timescale of ~1.5 s (Figure S7). As such, repeated illuminations could decrease the absorbance, which leads to the reduction in deflection after multiple cycles. When light irradiation is ceased, the DASA-polymer conjugate undergoes thermal reversion extremely slowly under ambient conditions (Supporting Information, Figure S7).

To further demonstrate the actuation capabilities of our material, a photothermally powered crawler was designed to exploit the bending motions of the DASA–PHMA/PI bilayer film under illumination to enable locomotion. The crawler consisted of a thin bilayer cantilever ($20 \text{ mm} \times 1.5 \text{ mm} \times 35 \mu \text{m}$, where the bilayer film consists of a 25 μm PI layer and 10 μm DASA–PHMA layer, identical to that described above) attached to a pair of asymmetric legs made of a polystyrene film ($5 \text{ mm} \times 1 \text{ mm} \times 200 \mu \text{m}$). The crawler is cyclically illuminated by 160 mW/cm^2 light intensity using a halogen lamp, and its motion is recorded as a function of time (Movie S1). When the bilayer is oriented with the DASA–PHMA layer on top, crawling motions with convex bending were observed (Figure 4a). During each cycle of illumination, the cantilever bends, causing the rear legs to retract. When the light is turned

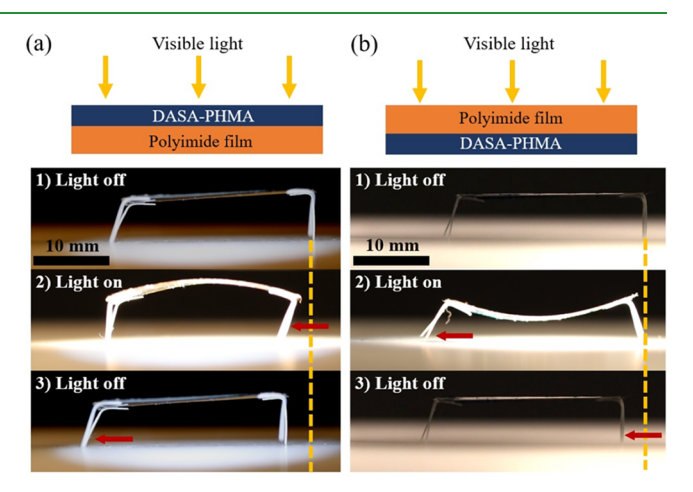


Figure 4. Demonstration of the application of a DASA-PHMA/PI bilayer film to form a remote-powered and controlled crawler. (a) Light-triggered convex bending motion is observed when DASA-PHMA and PI form the top and bottom layers, respectively. This leads to a robust, directional crawling motion, which can be described in three stages: (1) initial rest state before illumination, (2) backbone bending and rear foot dragging when the light is turned on, and (3) backbone relaxation, rear foot anchoring, and stretching when the light is turned off. (b) Inverted geometry, where the PI film forms the top layer, also endows locomotion capability, following same three motion stages but with concave bending and forefoot anchoring in each cycle.

off, the cantilever returns to its original shape, but the rear legs have anchored at their new position, causing the forelegs to extend and shifting the crawler center of mass to the left. If we construct a robot using an inverted specimen structure with the DASA-PHMA layer on top, we observe an inversion in the bending curvature but similar crawling performance (Figure 4b). In this case, the forelegs stretch first and anchor, and the

rear legs follow once the light has ceased. Moreover, the cyclic directional motion of the crawler under periodic illumination is robust regardless of the illumination spot position due to the photothermal nature of the actuation (Movie S2). Thus, the negatively photochromic DASA is an effective photoresponsive agent capable of generating robust photothermally driven mechanical output using low-intensity visible light, which can drive a locomotive crawling motion.

Finally, we sought to leverage DASA's negatively photochromic properties that shift the colored reactant to a colorless product to tune the magnitude of actuation. In contrast to tunable actuation using physical (i.e., structural patterning) or chemical (i.e., dynamic networks and acid patterning) triggers, the use of photochromic molecules that shift the absorption of the chromophore to a range outside of the excitation light source provides a novel noninvasive photochemical control mechanism. In the case of DASAs, by simply modulating irradiation time, the extent of bleaching can be controlled, and thus, the total amount of irradiant energy that can be converted to heat can be tuned. Figure 5a shows the corresponding color changes

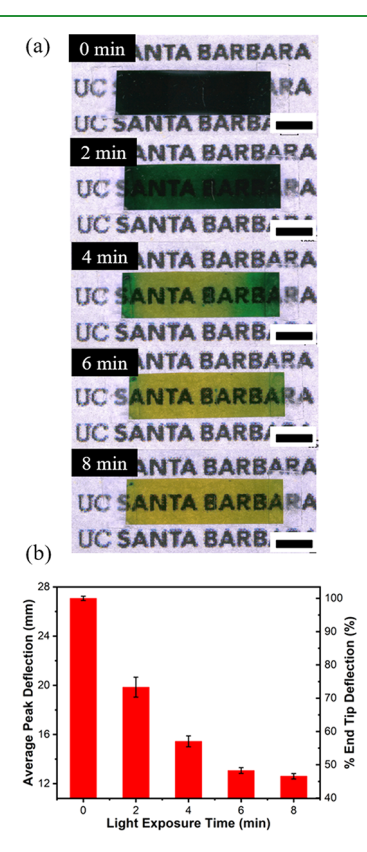


Figure 5. Photochemically tunable photothermal actuation of a DASA-PHMA/PI bilayer cantilever. (a) DASA-PHMA/PI cantilever changes color over light exposure time from dark green (open, top) to yellow (closed, bottom). In the closed form, the DASA-PHMA is clear and the yellow color is due to the PI film. (b) End tip deflection of DASA-PHMA/PI corresponding to the illumination time. Right-hand axis gives relative deflection, as compared to the initial state (0 min).

at different light exposure times from dark green (unswitched/open, 0 min) to yellow (fully switched/closed, 8 min), where the yellow color arises from the intrinsic color of the PI film, as the closed DASA is transparent/colorless. A pristine dark green cantilever composed of open DASA–PHMA records \sim 27.0 \pm 0.2 mm peak deflection at 160 mW/cm² irradiance with 5 mg

added weight. The peak deflection decreases as the cantilever decolorizes, and an identical transparent cantilever comprising closed DASA-PHMA records only \sim 12.1 \pm 0.2 mm peak deflection (Figure 5b). The enhanced actuation performance of the open-form DASA is expected, since the colored (open) DASA absorbs much more light energy, which is in turn dissipated as heat to the cantilever. Somewhat surprisingly, however, the DASA-PHMA/PI bilayer still actuates, achieving 46% of the peak deflection value recorded for the open-form DASA-PHMA/PI bilayer. Thermal imaging of the closed-form transparent bilayer under 160 mW/cm² illumination reveals a temperature increase of ~16.4 °C, which thus results in photothermal actuation (Figure S8). The ratio of temperature increases (0.42) between the open-form (\sim 39.2 °C, Figure 3d) and closed-form of the DASA-based cantilevers approximates the ratio of end tip deflections (0.45) for the same conditions, suggesting a direct correspondence between temperature difference and actuation performance. A control study of a single layer PI film also showed a temperature increase of ~13.5 °C under illumination, which indicates that the absorbance of PI is one of the heat generation sources (Figure S8).

It is possible to restore the bleached sample to its original state by exposure of the film in the closed form (transparent) to 75 $^{\circ}$ C for 1 min, which returns the sample to its open-form (colored) state. This reset sample can then be actuated again (Figure S9); however, the observed peak deflection amplitude is \sim 80% of the original deflection of the pristine sample, which we attribute to photodecomposition. Ongoing work aims to improve the reconfigurability by modifying the photoswitching properties in order to improve thermal reversion for multiple cycles and minimize the photothermal response of the bilayer system when DASA is in its closed, transparent form. However, this proof-of-principle study demonstrates that the negatively photochromic properties of DASA can be used to program the photothermal actuation in amorphous bilayer actuators and that the original state can be reset.

CONCLUSIONS

A modular synthetic strategy using Diels-Alder click chemistry was exploited to enable chemical incorporation of DASA into a load-bearing PHMA matrix. Cantilevers generated from this material demonstrate photochemically encoded tunable actuation as a result of the heat generated through their molecular absorbance. The photothermal actuation capabilities of DASA-PHMA were demonstrated by a cantilever lifting up to 13 times its weight under illumination and a centimeter-scale remotecontrolled crawler powered by robust light-activated bending. The negatively photochromic nature of DASA opens new possibilities for developing programmed actuators, "inching" the field toward smart soft robotics systems using broadband visible light. Future work will aim to leverage the tunability of the thermal half-life and excitation wavelength of DASAs to design programmable multiresponsive components with all-optical control for use in soft robotics.

MATERIALS AND METHODS

Methods. Unless stated otherwise, reactions were conducted under a nitrogen atmosphere using reagent-grade solvents. All commercially obtained reagents were used without purification, unless noted. Furfural was distilled before use and stored at $-18\,^{\circ}\text{C}$. All commercial vinyl monomers were purified by passing through a plug of basic alumina unless otherwise noted. Synthesis of polymer building blocks and DASA polymers was prepared in house (see the synthesis route in the

Supporting Information). Analytical thin-layer chromatography was carried out with Merck silica gel 60 F254 glass plates and visualized using a combination of UV and potassium permanganate staining or panisaldehyde. Flash column chromatography was performed with Merck silica gel 60 (70–230 mesh). All chromatographic solvents were of ACS grade and used without further purification. A 25 μ m-thick polyimide (Kapton, 2271 K-1) film without adhesive was purchased.

Characterization. ¹H NMR spectra were recorded on 400, 500, or 600 MHz spectrometers and ¹³C NMR spectra were recorded on 100, 125, or 150 MHz spectrometers. Differential scanning calorimetry (DSC) measurements were carried out using a Q2000 DSC V24.11 instrument from -80 to 100 °C at a heating rate of 10 °C/min and a cooling rate of 5 °C/min under a nitrogen flow of 50 mL/min. The second heating/cooling cycle was analyzed to measure the glasstransition temperature of the specimen. The photoinduced optical absorption kinetics were measured using a custom pump-probe system described in the Supporting Information. Thermomechanical analysis was performed in the Cornell Center for Materials Research at Cornell University, NY, USA to determine the coefficients of thermal expansion of the DASA-PHMA and PI films. Wide-angle X-ray scattering (WAXS) measurements were conducted in transmission mode using a custom-constructed X-ray diffractor. The WAXS instrument utilized a Cu target X-ray source (1.54 Å) with parallel beam multilayer optics and monochromator, high-efficiency scatterless hybrid slit collimator developed in house, and Pilatus100K and Eiger 1M solid-state detectors. The thicknesses of each layer of the bilayer films were measured using a scanning electron microscopy instrument at an accelerating voltage of 2 kV in secondary electron mode. UV-vis absorption spectra were recorded on a UV-vis spectrometer from 200 to 1200 nm wavelengths. For mass spectroscopy, a high-resolution time-of-flight mass spectrometer equipped with electron ionization, chemical ionization, and field ionization/field desorption ion sources was used.

Deflection Measurement. Cantilever motion during actuation was captured by a Canon EOS Rebel T5i camera (100 mm f/2.8 macro lens, magnification 1x) at a 30 Hz frame rate. A halogen lamp (EKW 150 W) coupled with a fiber optic illuminator was used. Light irradiance calibration was conducted using an optical power meter connected to a high-power detector (detail was provided in the Supporting Information). Irradiance was controlled by varying the distance between the detector and the fiber optic illuminator end tip. Peak deflection at each illumination cycle was measured by tracking the position of the end tip of the cantilever at every frame using the ImageJ software and selecting the maximum difference between before and under irradiation. Three specimens were used at all irradiances. Average peak deflection was obtained by averaging peak deflections of 15 total cycles at each irradiance per specimen. Temporal deflection traces were measured by MATLAB. The recorded video images were converted to binary images using MATLAB. The tip position of the cantilever was extracted from each binary frame using the custom-written MATLAB code for detection and tracking. An infrared camera (FLIR E60) was used to record the temperature of the bilayer cantilever under illumination. The built-in spot meter was used to select the center of the illuminated specimen and to measure the temperature of that region in each frame.

Sample Preparation. The DASA-PHMA/PI bilayer film was prepared by drop casting. The DASA-PHMA polymer was dissolved in THF solvent to a concentration of 10 mg/mL in a vial and sonicated in a water bath for 15 min The commercially obtained PI film was cut using a razor and attached by a double-sided adhesive tape to the bottom of the mold that has a 1 mm-thick \times 25 mm \times 8 mm rectangular hole into which 200 μ L of the sonicated DASA-PHMA solution was deposited. The mold containing the sample was then placed in a vacuum chamber (3625A, Thermo Scientific) to promote the evaporation of the solvent. The vacuum level was optimized by adjusting a manual knob attached to the chamber to produce the best-quality film. During each evaporation process, four sheets of the DASA-PHMA film were prepared. Thin-film DASA-PHMA (ca. 800 nm thick) samples were prepared by spin coating on a microscope glass slide, as follows. A 10 mg/mL DASA-PHMA solution in chloroform was prepared in a vial

and sonicated at room temperature (20 °C) for 15 min. Glass substrates $(25 \text{ mm} \times 25 \text{ mm} \times 1 \text{ mm-thick})$ were prepared by cutting a 25 mm \times 75 mm microscope glass slide using a glass cutter, followed by cleaning with ethanol and acetone in a sonication bath for 10 min each and then cleaning with DI water. Slides were treated with ozone plasma (Novascan ozone cleaner) for 10 min. DASA-PHMA films were prepared by spin coating at 2000 rpm for 45 s. The thin-film specimens were stored in a vacuum chamber for 24 h to remove residual solvent by evaporation.

ASSOCIATED CONTENT

Supporting Information

The Supporting Information is available free of charge at https://pubs.acs.org/doi/10.1021/acsami.0c15116.

Detailed information regarding syntheses, material characterization, actuation test, instrumentation, and data not included in the main text (PDF)

Crawling via a convex bending motion (MP4)

Illumination on the right and left of the cantilever (MP4)

AUTHOR INFORMATION

Corresponding Authors

Megan T. Valentine – Department of Mechanical Engineering, University of California-Santa Barbara, Santa Barbara, California 93106, United States; o orcid.org/0000-0003-4781-8478; Email: valentine@engineering.ucsb.edu

Javier Read de Alaniz - Department of Chemistry and Biochemistry, University of California-Santa Barbara, Santa Barbara, California 93106, United States; o orcid.org/ 0000-0003-2770-9477; Email: javier@chem.ucsb.edu

Authors

Jaejun Lee - Department of Chemistry and Biochemistry and Department of Mechanical Engineering, University of California-Santa Barbara, Santa Barbara, California 93106, **United States**

Miranda M. Sroda - Department of Chemistry and Biochemistry, University of California-Santa Barbara, Santa Barbara, California 93106, United States

Younghoon Kwon – Department of Mechanical Engineering, University of California-Santa Barbara, Santa Barbara, California 93106, United States

Sara El-Arid – Department of Chemistry and Biochemistry, University of California-Santa Barbara, Santa Barbara, California 93106, United States

Serena Seshadri – Department of Chemistry and Biochemistry, University of California-Santa Barbara, Santa Barbara, California 93106, United States

Luke F. Gockowski – Department of Mechanical Engineering, University of California-Santa Barbara, Santa Barbara, California 93106, United States

Elliot W. Hawkes – Department of Mechanical Engineering, University of California-Santa Barbara, Santa Barbara, California 93106, United States

Complete contact information is available at: https://pubs.acs.org/10.1021/acsami.0c15116

Author Contributions

§J.L. and M.M.S. contributed equally to this work.

The authors declare no competing financial interest. M.T.V. and J.R.D.A. jointly supervised the work.

ACKNOWLEDGMENTS

This work was primarily supported by the U.S. Army Research Office under Cooperative Agreement W911NF-19-2-0026 for the Institute for Collaborative Biotechnologies. Views and conclusions are those of the authors and should not be interpreted as representing official policies, either expressed or implied, of the U.S. Government. Support was also provided by the Office of Naval Research through the MURI on Photomechanical Material Systems through grant no. ONR N00014-18-1-2624 and National Science Foundation (NSF) through grant no. EFMA 1935327. M.M.S. was supported by the UCSB Graduate Opportunity Fellowship. Y.K. and L.F.G. were partially supported by the MRSEC Program of the National Science Foundation through grant no. DMR-1720256 (IRG-3). The authors acknowledge the use of the Microfluidics Laboratory within the California NanoSystems Institute, supported by the University of California, Santa Barbara and the University of California, Office of the President, and the MRL Shared Experimental Facilities supported by the MRSEC Program of the NSF under award no. DMR 1720256, a member of the NSF-funded Materials Research Facilities Network (www. mrfn.org). The authors thank Dr. Alexander Mikhailovsky for his help in constructing the optical setup used for the switching experiment. The authors acknowledge the use of the Cornell Center for Materials Research Shared Facilities, which are supported through the NSF MRSEC program (DMR-1719875).

REFERENCES

- (1) Pei, Z.; Yang, Y.; Chen, Q.; Terentjev, E. M.; Wei, Y.; Ji, Y. Mouldable Liquid-Crystalline Elastomer Actuators with Exchangeable Covalent Bonds. *Nat. Mater.* **2014**, *13*, 36–41.
- (2) Chen, L.; Weng, M.; Zhou, P.; Zhang, L.; Huang, Z.; Zhang, W. Multi-Responsive Actuators Based on a Graphene Oxide Composite: Intelligent Robot and Bioinspired Applications. *Nanoscale* **2017**, *9*, 9825–9833.
- (3) He, S.; Chen, P.; Qiu, L.; Wang, B.; Sun, X.; Xu, Y.; Peng, H. A Mechanically Actuating Carbon-Nanotube Fiber in Response to Water and Moisture. *Angew. Chem., Int. Ed.* **2015**, *54*, 14880–14884.
- (4) Shim, T. S.; Kim, S.-H.; Heo, C.-J.; Jeon, H. C.; Yang, S.-M. Controlled Origami Folding of Hydrogel Bilayers with Sustained Reversibility for Robust Microcarriers. *Angew. Chem., Int. Ed.* **2012**, *51*, 1420–1423.
- (5) Yu, Y.; Nakano, M.; Ikeda, T. Directed Bending of a Polymer Film by Light. *Nature* **2003**, 425, 145–145.
- (6) Camacho-Lopez, M.; Finkelmann, H.; Palffy-Muhoray, P.; Shelley, M. Fast Liquid-Crystal Elastomer Swims into the Dark. *Nat. Mater.* **2004**, *3*, 307–310.
- (7) Kohlmeyer, R. R.; Chen, J. Wavelength-Selective, Ir Light-Driven Hinges Based on Liquid Crystalline Elastomer Composites. *Angew. Chem., Int. Ed.* **2013**, *52*, 9234–9237.
- (8) Islam, M. R.; Li, X.; Smyth, K.; Serpe, M. J. Polymer-Based Muscle Expansion and Contraction. *Angew. Chem., Int. Ed.* **2013**, *52*, 10330–10333.
- (9) Qian, X.; Chen, Q.; Yang, Y.; Xu, Y.; Li, Z.; Wang, Z.; Wu, Y.; Wei, Y.; Ji, Y. Untethered Recyclable Tubular Actuators with Versatile Locomotion for Soft Continuum Robots. *Adv. Mater.* **2018**, *30*, 1801103.
- (10) White, T. J.; Tabiryan, N. V.; Serak, S. V.; Hrozhyk, U. A.; Tondiglia, V. P.; Koerner, H.; Vaia, R. A.; Bunning, T. J. A High Frequency Photodriven Polymer Oscillator. *Soft Matter* **2008**, *4*, 1796–1798.
- (11) Ryabchun, A.; Li, Q.; Lancia, F.; Aprahamian, I.; Katsonis, N. Shape-Persistent Actuators from Hydrazone Photoswitches. *J. Am. Chem. Soc.* **2019**, 141, 1196–1200.

- (12) Aßhoff, S. J.; Lancia, F.; Iamsaard, S.; Matt, B.; Kudernac, T.; Fletcher, S. P.; Katsonis, N. High-Power Actuation from Molecular Photoswitches in Enantiomerically Paired Soft Springs. *Angew. Chem., Int. Ed.* **2017**, *56*, 3261–3265.
- (13) Boelke, J.; Hecht, S. Designing Molecular Photoswitches for Soft Materials Applications. *Adv. Opt. Mater.* **2019**, *7*, 1900404.
- (14) Jiang, W.; Niu, D.; Liu, H.; Wang, C.; Zhao, T.; Yin, L.; Shi, Y.; Chen, B.; Ding, Y.; Lu, B. Photoresponsive Soft-Robotic Platform: Biomimetic Fabrication and Remote Actuation. *Adv. Funct. Mater.* **2014**, 24, 7598–7604.
- (15) Ma, H.; Hou, J.; Wang, X.; Zhang, J.; Yuan, Z.; Xiao, L.; Wei, Y.; Fan, S.; Jiang, K.; Liu, K. Flexible, All-Inorganic Actuators Based on Vanadium Dioxide and Carbon Nanotube Bimorphs. *Nano Lett.* **2017**, 17, 421–428.
- (16) Lu, X.; Zhang, H.; Fei, G.; Yu, B.; Tong, X.; Xia, H.; Zhao, Y. Liquid-Crystalline Dynamic Networks Doped with Gold Nanorods Showing Enhanced Photocontrol of Actuation. *Adv. Mater.* **2018**, *30*, 1706597
- (17) Kuenstler, A. S.; Kim, H.; Hayward, R. C. Liquid Crystal Elastomer Waveguide Actuators. *Adv. Mater.* **2019**, *31*, 1901216.
- (18) Ube, T.; Kawasaki, K.; Ikeda, T. Photomobile Liquid-Crystalline Elastomers with Rearrangeable Networks. *Adv. Mater.* **2016**, 28, 8212—8217.
- (19) Gelebart, A. H.; Mulder, D. J.; Vantomme, G.; Schenning, A. P. H. J.; Broer, D. J. A Rewritable, Reprogrammable, Dual Light-Responsive Polymer Actuator. *Angew. Chem., Int. Ed.* **2017**, *56*, 13436–13439.
- (20) Gelebart, A. H.; Vantomme, G.; Meijer, E. W.; Broer, D. J. Mastering the Photothermal Effect in Liquid Crystal Networks: A General Approach for Self-Sustained Mechanical Oscillators. *Adv. Mater.* **2017**, *29*, 1606712.
- (21) Gelebart, A. H.; Jan Mulder, D.; Varga, M.; Konya, A.; Vantomme, G.; Meijer, E. W.; Selinger, R. L. B.; Broer, D. J. Making Waves in a Photoactive Polymer Film. *Nature* **2017**, *546*, 632–636.
- (22) Qian, X.; Zhao, Y.; Alsaid, Y.; Wang, X.; Hua, M.; Galy, T.; Gopalakrishna, H.; Yang, Y.; Cui, J.; Liu, N.; Marszewski, M.; Pilon, L.; Jiang, H.; He, X. Artificial Phototropism for Omnidirectional Tracking and Harvesting of Light. *Nat. Nanotechnol.* **2019**, *14*, 1048–1055.
- (23) Yoshida, R.; Ueki, T. Evolution of Self-Oscillating Polymer Gels as Autonomous Polymer Systems. *NPG Asia Mater.* **2014**, *6*, e107–e107
- (24) Hendrikx, M.; ter Schiphorst, J.; van Heeswijk, E. P. A.; Koçer, G.; Knie, C.; Bléger, D.; Hecht, S.; Jonkheijm, P.; Broer, D. J.; Schenning, A. P. H. J. Re- and Preconfigurable Multistable Visible Light Responsive Surface Topographies. *Small* **2018**, *14*, 1803274.
- (25) Deng, J.; Li, J.; Chen, P.; Fang, X.; Sun, X.; Jiang, Y.; Weng, W.; Wang, B.; Peng, H. Tunable Photothermal Actuators Based on a Pre-Programmed Aligned Nanostructure. *J. Am. Chem. Soc.* **2016**, *138*, 225–230.
- (26) Cheng, Y.-C.; Lu, H.-C.; Lee, X.; Zeng, H.; Priimagi, A. Kirigami-Based Light-Induced Shape-Morphing and Locomotion. *Adv. Mater.* **2020**, 32, 1906233.
- (27) Lahikainen, M.; Zeng, H.; Priimagi, A. Reconfigurable Photoactuator through Synergistic Use of Photochemical and Photothermal Effects. *Nat. Commun.* **2018**, *9*, 4148.
- (28) Vapaavuori, J.; Bazuin, C. G.; Priimagi, A. Supramolecular Design Principles for Efficient Photoresponsive Polymer—Azobenzene Complexes. *J. Mater. Chem. C* **2018**, *6*, 2168—2188.
- (29) Helmy, S.; Leibfarth, F. A.; Oh, S.; Poelma, J. E.; Hawker, C. J.; Read de Alaniz, J. Photoswitching Using Visible Light: A New Class of Organic Photochromic Molecules. *J. Am. Chem. Soc.* **2014**, *136*, 8169—8172
- (30) Helmy, S.; Oh, S.; Leibfarth, F. A.; Hawker, C. J.; Read de Alaniz, J. Design and Synthesis of Donor–Acceptor Stenhouse Adducts: A visible Light Photoswitch Derived from Furfural. *J. Org. Chem.* **2014**, 79, 11316–11329.
- (31) Lerch, M. M.; Szymański, W.; Feringa, B. L. The (Photo)-Chemistry of Stenhouse Photoswitches: Guiding Principles and System Design. *Chem. Soc. Rev.* **2018**, *47*, 1910–1937.

- (32) Han, B.; Zhang, Y.-L.; Chen, Q.-D.; Sun, H.-B. Carbon-Based Photothermal Actuators. Adv. Funct. Mater. 2018, 28, 1802235.
- (33) Hemmer, J. R.; Poelma, S. O.; Treat, N.; Page, Z. A.; Dolinski, N. D.; Diaz, Y. J.; Tomlinson, W.; Clark, K. D.; Hooper, J. P.; Hawker, C.; Read de Alaniz, J. Tunable Visible and near Infrared Photoswitches. *J. Am. Chem. Soc.* **2016**, *138*, 13960–13966.
- (34) Ulrich, S.; Hemmer, J. R.; Page, Z. A.; Dolinski, N. D.; Rifaie-Graham, O.; Bruns, N.; Hawker, C. J.; Boesel, L. F.; Read de Alaniz, J. Visible Light-Responsive Dasa-Polymer Conjugates. *ACS Macro Lett.* **2017**, *6*, 738–742.
- (35) Hemmer, J. R.; Page, Z. A.; Clark, K. D.; Stricker, F.; Dolinski, N. D.; Hawker, C. J.; Read de Alaniz, J. Controlling Dark Equilibria and Enhancing Donor—Acceptor Stenhouse Adduct Photoswitching Properties through Carbon Acid Design. J. Am. Chem. Soc. 2018, 140, 10425—10429.
- (36) Seshadri, S.; Gockowski, L. F.; Lee, J.; Sroda, M.; Helgeson, M. E.; Read de Alaniz, J.; Valentine, M. T. Self-Regulating Photochemical Rayleigh-Bénard Convection Using a Highly-Absorbing Organic Photoswitch. *Nat. Commun.* **2020**, *11*, 2599.
- (37) Powell, A. W.; Stavrinadis, A.; Christodoulou, S.; Quidant, R.; Konstantatos, G. On-Demand Activation of Photochromic Nanoheaters for High Color Purity 3D Printing. *Nano Lett.* **2020**, *20*, 3485–3491.
- (38) St. Amant, A. H.; Discekici, E. H.; Bailey, S. J.; Zayas, M. S.; Song, J.-A.; Shankel, S. L.; Nguyen, S. N.; Bates, M. W.; Anastasaki, A.; Hawker, C. J.; Read de Alaniz, J. Norbornadienes: Robust and Scalable Building Blocks for Cascade "Click" Coupling of High Molecular Weight Polymers. J. Am. Chem. Soc. 2019, 141, 13619–13624.
- (39) Chen, Q.; Diaz, Y. J.; Hawker, M. C.; Martinez, M. R.; Page, Z. A.; Xiao-An Zhang, S.; Hawker, C. J.; Read de Alaniz, J. Stable Activated Furan and Donor—Acceptor Stenhouse Adduct Polymer Conjugates as Chemical and Thermal Sensors. *Macromolecules* **2019**, *52*, 4370—4375.
- (40) Sinawang, G.; Wu, B.; Wang, J.; Li, S.; He, Y. Polystyrene Based Visible Light Responsive Polymer with Donor—Acceptor Stenhouse Adduct Pendants. *Macromol. Chem. Phys.* **2016**, 217, 2409—2414.
- (41) Yap, J. E.; Mallo, N.; Thomas, D. S.; Beves, J. E.; Stenzel, M. H. Comparing Photoswitching of Acrylate or Methacrylate Polymers Conjugated with Donor—Acceptor Stenhouse Adducts. *Polym. Chem.* **2019**, *10*, 6515—6522.
- (42) Priimagi, A.; Cattaneo, S.; Ras, R. H. A.; Valkama, S.; Ikkala, O.; Kauranen, M. Polymer—Dye Complexes: A Facile Method for High Doping Level and Aggregation Control of Dye Molecules. *Chem. Mater.* **2005**, *17*, 5798–5802.
- (43) Kaczmarek, H.; Kamińska, A.; van Herk, A. Photooxidative Degradation of Poly(Alkyl Methacrylate)S. *Eur. Polym. J.* **2000**, *36*, 767–777.
- (44) Child, W. C., Jr.; Ferry, J. D. Dynamic Mechanical Properties of Poly-N-Hexyl Methacrylate. *J. Colloid Sci.* **195**7, *12*, 389–399.
- (45) Lui, B. F.; Tierce, N. T.; Tong, F.; Sroda, M. M.; Lu, H.; Read de Alaniz, J.; Bardeen, C. J. Unusual Concentration Dependence of the Photoisomerization Reaction in Donor—Acceptor Stenhouse Adducts. *Photochem. Photobiol. Sci.* **2019**, *18*, 1587—1595.
- (46) Yakacki, C. M.; Saed, M.; Nair, D. P.; Gong, T.; Reed, S. M.; Bowman, C. N. Tailorable and Programmable Liquid-Crystalline Elastomers Using a Two-Stage Thiol—Acrylate Reaction. *RSC Adv.* **2015**, *5*, 18997—19001.
- (47) White, T. J. Photomechanical Effects in Liquid Crystalline Polymer Networks and Elastomers. *J. Polym. Sci., Part B: Polym. Phys.* **2018**, *56*, 695–705.
- (48) Timoshenko, S. Analysis of Bi-Metal Thermostats. J. Opt. Soc. Am. 1925, 11, 233–255.